

2.5 Small Amplitude Vibration of Sagged Cables

2.5.1 Stationary Sagged Cables

Irvine and Caughey[1974], Irvine[1981] trace the historical development of sagged cables, and conclude that by the early 1800's correct solutions had been achieved for the limiting cases of catenaries, namely taut strings and vertically hanging cables. However, the intermediate condition had not been solved. The symmetric modes of flat sagged cables where the sag to span ratio was neither zero nor infinite was analysed initially by Rohrs(1851)[1851] and Routh(1868)[1884]. Both authors assumed inextensible cable behaviour, thus solving the wave equation subject to a constraint condition. The resulting solutions applied essentially to situations where the catenary stiffness associated with its geometric profile is low compared to the axial stiffness of the cable element. Although solutions for the limiting conditions of the cable were established, no single theory could describe the transition continuously between deep sag cable behaviour and the limiting case of the taut string. Specifically, the modal characteristics of the symmetric modes of flat sag and deep sag cables were at that stage known to be governed by the roots of the frequency equations, cited respectively as:

$$\cos(\frac{1}{2}\beta l) = 0$$

$$\tan(\frac{1}{2}\beta l) = \frac{1}{2}\beta l$$

Where $\beta = (m\omega^2/H)^{\frac{1}{2}}$. The roots of the above equations are vastly different, where the first root of each equation is π and 2.86π respectively. This difference reflects the fact that in the limiting condition of a flat sag cable, the taut string, the fundamental mode is symmetric with respect to the midspan, whilst in the case of the deep sag cable, the fundamental is antisymmetric with respect to the midspan. Irvine and Caughey[1974] note that the assumption of inextensible cable behaviour is unrealistic when considering a cable where the sag tends to zero, since any deformation would necessitate elastic stretch. By allowing for elastic stretch, Irvine and Caughey[1974] demonstrated that a consistent theory could be developed describing the transition from deep sag to taut string behaviour.

The aerodynamic failure of Tacoma Narrows bridge in 1940 prompted further research into cable dynamics. Pugsley[1949], Saxon and Cahn[1953], Goodey[1961], developed the deep sag inextensible cable theory further. However, it was only when cable elasticity was accounted for that the dynamic behaviour of a cable could adequately be described in the transition region between that of the taut flat string to the deep sag profile. Laasonen[1959] and later Soler[1970] presented an analysis whereby cable elasticity was accounted for, and identified a dimensionless parameter, which Irvine and Caughey⁴[1974] later termed the cable parameter, λ^2 . Irvine and Caughey [1974] demonstrated that this single parameter was sufficient to describe the transition between taut string and deep sag cable behaviour. A brief development of the theory pertaining to the dynamic characteristics of small amplitude sagged cables is presented below.

Irvine and Caughey [1974] demonstrated that by considering small amplitude oscillations w from the equilibrium profile of the cable z , and accounting only for first order terms, the in-plane equation of motion of a shallow sag cable reduced to:

$$H \frac{\partial^2 w}{\partial x^2} + h \frac{\partial^2 z}{\partial x^2} = m \frac{\partial^2 w}{\partial t^2} \quad (2.5)$$

Where m represents the mass per unit length, and h represents the additional component of the horizontal tension generated during the motion, which is given to first order as:

$$\frac{hL_z}{EA} = \frac{mg}{H} \int_0^l w dx \quad (2.6)$$

It is pertinent to note that the term $\frac{\partial^2 z}{\partial x^2}$ in equation (2.5) represents to first order the curvature of the cable in its equilibrium configuration. Employing the argument introduced previously, equation (2.6) confirms that no additional tension is generated in the cable during the oscillation, if the mode shape, or displacement w from the equilibrium profile is antisymmetric about the mid-plane of the span. Thus it is clear, that the equation of motion (2.5) reduces to that of the wave equation for antisymmetric modes, and consequently, to first order the curvature of the cable does not influence the natural frequency.

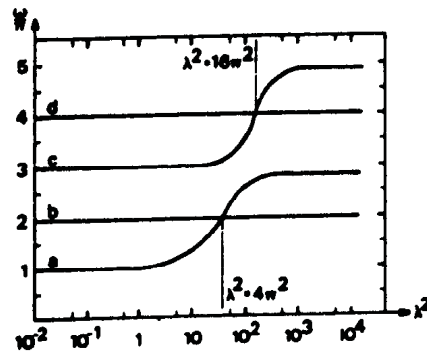
⁴Laasonen's[1959] results are equivalent to those of Irvine and Caughey[1974], however the latter formulated the problem in a more physical sense, which perhaps explains why so little reference is made to Laasonen.

Conversely, symmetric mode shapes introduce tension changes due to geometric adjustment during the oscillation, and consequently cable curvature can significantly affect the natural frequency of symmetric modes.

Since the cable profile was assumed shallow, an approximate quadratic cable profile for z may be utilised and substituted into equation (2.5). In this instance the curvature is constant, and the equation of motion may be solved to obtain w as a function of h . Substituting the solution for w into equation (2.6), results in a transcendental characteristic equation, the roots of which represent the linear natural frequencies of the cable, spanning all configurations from a taut string to a deep sag cable⁵.

$$\tan \frac{\bar{\omega}}{2} = \frac{\bar{\omega}}{2} - \frac{4}{\lambda^2} \left(\frac{\bar{\omega}}{2} \right)^3 \quad (2.7)$$

Where $\bar{\omega} = \omega l / (H/m)^{1/2}$, and $\lambda^2 = (mgl/H)^2 l / (HL_e/EA)$. The dependence of the characteristic equation on the cable parameter λ^2 is clearly demonstrated. The limiting configurations of $\lambda^2 \approx 0, \infty$ represent the taut string and deep sag cable respectively. The dependence of the natural frequencies on λ^2 is illustrated in figure 2.3.



3.3 General dimensionless curves for the first four natural frequencies of a flat-sag suspended cable: (a) first symmetric in-plane mode, (b) first antisymmetric in-plane mode, (c) second symmetric in-plane mode, (d) second antisymmetric in-plane mode.

Figure 2.3: Irvine (1981): In-plane natural frequencies of a cable.

With reference to figure 2.3, it is evident that the antisymmetric modes are independent of λ , and equivalent to those of a taut string. The symmetric modes however change significantly as λ increases with increasing sag or cable

⁵This frequency equation is identical to that derived by Laasonen [1959].

curvature, resulting in a modal cross-over or mode reversion, after which the antisymmetric mode becomes the fundamental in-plane mode of a deep sag cable. Irvine[1981] also considered the case of a cable inclined at an angle θ to the horizontal plane, and concluded that if the cable parameter were modified to account for the angle of inclination, $\lambda_1^2 = (mg/\cos\theta/H)^2/(HL_c/EA)$, then the results presented in figure 2.3 would apply. This result is not strictly correct, since the asymmetry of the mode shapes associated with inclined cables causes frequency veering as opposed to modal cross-over.

Iyengar and Rao[1988] presented a study of the natural frequencies of a sagged cable under a constant lateral load. In this case the equilibrium profile is non-planar, and hence curvature coupling exists between the in- and out-of-plane equations of motion. The stability of the cable due to an additional periodic lateral load was considered. The emphasis of this analysis was clearly directed at power transmission lines. Rao and Iyengar[1991] extended this analysis to examine the response of a shallow sag cable in its first symmetric in-plane and out-of-plane mode, due to forced harmonic excitation in the in-plane and a uniform static load in the out-of-plane directions. A special case of tuning was chosen such that the first symmetric in-plane mode tuned to twice the first symmetric out-of-plane mode, and hence an internal resonance of 2:1 existed, coupling the response between the in-plane and out-of-plane symmetric modes. Simultaneously an in-plane external resonance was induced. The tuning of the internal resonance was dependent on the cable curvature, and hence the quadratic nonlinearities present in the system. By comparing the response of the system due to an external resonance, with and without internal resonance, it was concluded that cable curvature and hence the quadratic nonlinearity has a significant effect on the system response. The stability analysis of the system confirmed that regions existed where steady state periodic motion did not exist.

In a similar fashion to the analyses of Lubkin and Stoker[1943], Tagata[1977, 1983], Takahashi[1991] examined the stability of flat-sag cables to periodic axial excitation. The sag to span ratio was varied to span the first modal cross-over region. It was demonstrated that the widths of the unstable regions were affected by the sag to span ratio in the regions of modal cross-over, and that combination parametric resonances arose. Perkins[1992b] showed that the equations of motion applied by Takahashi[1991] were inconsistent, leading to erroneous conclusions. Perkins[1992b] showed that such a configuration resulted in parametric as well as external excitation, and that combination parametric resonances did not arise.

2.5.2 Travelling Sagged Cables

Simpson[1972] investigated the in-plane free vibration of a horizontal travelling elastic catenary. The equations of motion were derived by generalising the equations of a static catenary. Simpson's[1972] analysis considered a catenary with a sag to span ratio of 1:20. Through a process of linearisation of the nonlinear equations of motion, Simpson [1972] confirmed previous results pertaining to flat travelling strings, and demonstrated the influence of cable curvature on the natural frequencies. Simpson's [1972] results indicated that frequency coalescence between modes may occur, as well as mode reversion, whereby a higher order mode reverts to the shape of a lower order mode for certain axial velocities.

More recent analyses by Triantafyllou[1985], Perkins and Mote[1987] have reconsidered the problem of cables with initial sag translating between arbitrarily inclined eyelets. Triantafyllou[1985] presented an analysis which considered the case of small sag and large sag translating cables. His analysis confirmed the results of Simpson[1972], and provided further explanation to the occurrence of mode reversion and frequency coalescence. The results indicated that for small sag horizontal cables, the phenomenon of mode reversion and frequency coalescence occurred, whereas when the cable was inclined, frequency coalescence was replaced by frequency avoidance or veering, where the frequencies approach closely but are distinct. Also, only partial mode reversion occurs, where the mode shapes become hybrid combinations of symmetric and antisymmetric modes. Perkins and Mote [1987] derived the three dimensional equations of motion for an arbitrarily sagged translating cable based on a finite strain approach and conservation of cable mass. On linearising the equations of motion, they demonstrated that the phenomenon of frequency coalescence is conditional on the symmetry of the mode shapes, and thus frequency veering as opposed to coalescence occurs for both translating cables and inclined cables, as the mode shapes become asymmetrical. The results of the analysis were compared with those of Simpson [1972] for a horizontal small sag translating cable, and with those of Irvine and Caughey [1974] for stationary cables. It was demonstrated that the results confirmed those of Simpson [1972], except that frequency crossings were replaced by veerings, and those of Irvine and Caughey[1974], except at extreme values of the cable parameter λ^2 . The large difference at small values of λ^2 was attributed to the modal interaction of longitudinal modes with lateral modes, not accommodated by Irvine and Caughey's[1974] derivation which assumed quasi-static stretch in the longitudinal direction. The divergence of the behaviour was accentuated by varying the cable elasticity, thus in practice with steel wire ropes, this behaviour is associated with higher transverse modes, where longitudinal/ lateral

modal interaction is more significant. Perkins and Mote [1987] noted in this study that a second stable equilibrium profile could exist, after the divergence and buckling of the stable catenary at speeds greater than the lateral wave speed. This concept was developed further, Perkins and Mote[1989], and confirmed experimentally. Burges and Triantafyllou[1988] investigated the aspect of longitudinal and lateral modal interaction further. They examined stationary small sag horizontal and inclined cables. Modal interaction between the first elastic or longitudinal mode and the higher (18-22) transverse modes was considered. It was demonstrated that longitudinal interaction promoted the phenomena of frequency coalescence and avoidance in the horizontal case, whereas only avoidance occurred in the inclined case.

The results obtained by Perkins and Mote are presented in figure 2.4, and figure 2.5., where a comparison between those of Irvine and Caughey[1974] for a stationary sagged cable, and those of Simpson[1972] for a translating cable with a sag to span ratio of 1:20, is presented respectively.

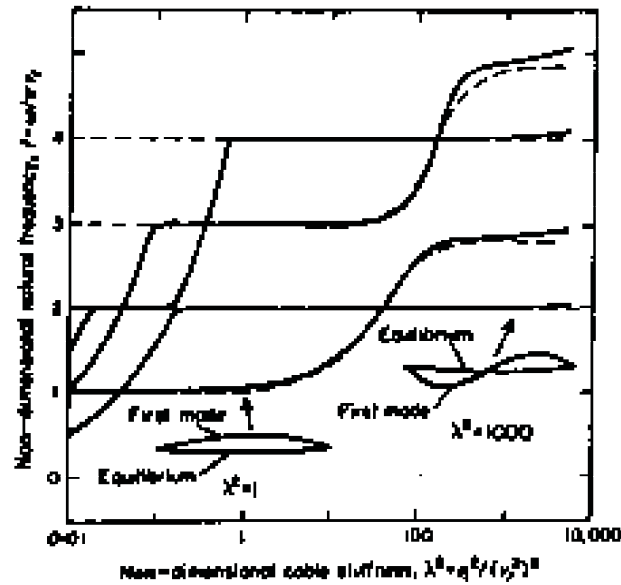


Figure 4. Comparison with Irvine's theory for the case $v_1^2 = 5$. Irvine's results are reproduced from reference [6] and reported in the units used in references [3,6]. The first mode shape is shown for $\lambda^2 = 1$ and 1000. —, Cable model; ---, Irvine.

Figure 2.4: Perkins and Mote (1987): In-plane natural frequencies of a cable - Comparison with Irvine's theory.

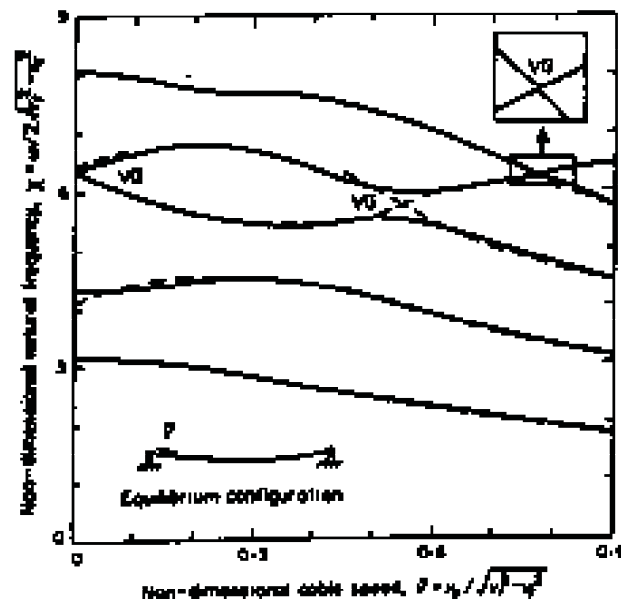


Figure 5. Comparison with Simpson's theory. In-plane frequencies for a travelling cable having horizontal eyelets and equilibrium sag to span ratio 0.050. Simpson's results are reproduced from reference [14] and based on Simpson's parameters: $s = 0.4 = 1/4(v_1^2 - v_2^2)$ and $\mu = 0.001 = (v_1^2 - v_2^2)/v_1^2$. —, Cable model; - - -, Simpson; VCI, veering.

Figure 2.5: Perkins and Mote (1987): In-plane natural frequencies of a translating cable - Comparison with Simpson's theory.

2.6 Large Amplitude Vibration of Sagged Cables

Luogno, Rega and Vestroni[1982] defined a simplified two degree of freedom model for transverse in-plane and out-of-plane motion of a sagged cable. The purpose of the study was to demonstrate monofrequent in-plane and out-of-plane oscillation. As defined by Luogno et al[1982], monofrequent oscillations occur when one of the normal displacement co-ordinates prevails over the others, and all points move with a frequency that is equal to or a multiple of the nonlinear frequency of that co-ordinate. Thus monofrequent oscillations reduce to the modal oscillations of the linear system, as the nonlinearity vanishes. This provides a convenient basis for ascertaining the influence of system parameters on the nonlinear frequency amplitude relationship. The equations of motion developed contained both quadratic and cubic nonlinearities, associated with the curvature and stretch of the cable respectively. The initial conditions required to induce in-plane (extensional) and out-of-plane (pendulum type) monofrequent oscillations were determined. It was shown that in-plane or extensional monofrequent oscillations could be induced for any tuning of the in- and out-of-plane modes, conversely out-of-plane monofrequent oscillations could only be induced in the absence of internal resonance. With regard to the in-plane motion, it was demonstrated that the nonlinearities, and the amplitude of the induced motion strongly influenced the nonlinear frequencies of the cable. Drift of the midpoint of the in-plane oscillations occurred due to the quadratic nature of the nonlinearity related to cable curvature. The variation of the nonlinear frequency from the linear frequency depended strongly on the cable parameters, where a softening behaviour was observed as the cable curvature increased, whilst hardening behaviour occurred as the cable approached a taut string. The importance of internal resonance was demonstrated with respect to the out-of-plane or pendulum type monofrequent oscillations, which depended strongly on the degree of tuning between the symmetric in- and out-of-plane modes. The internal resonance condition (where the first symmetric in-plane mode tunes to twice the first symmetric out-of-plane mode at a modal cross-over as defined by Irvine and Caughey[1974]) divided the system behaviour between a hardening or softening type.

Rega, Vestroni and Benedettini[1984], examined the planar response of a sagged cable with sag to span ratios of less than $1/8$, where the amplitude of response was sufficiently large to necessitate the inclusion of higher order nonlinearities. The spatial variable was eliminated from the partial differential equations of motion by using the linear eigenfunctions of a shallow sag cable, and applying an integral formulation. The resulting equations of motion reflected both quadratic and cubic nonlinearities; the quadratic nonlinearity is induced by

the cable curvature and thus the ability of the cable to absorb additional tension by geometric adjustment of the profile. The cubic nonlinearity reflects the additional tension generated via second order stretch of the cable. These terms are related to the first and second integral on the right hand side of equation 2.2. The equation pertinent to the temporal domain was thus cast in the form:

$$\ddot{q} + q + c_2 q^2 + c_3 q^3 = Q(t)$$

Since the quadratic coefficient is a consequence of the cables ability to absorb additional tension through geometric adjustment of the profile, which vanishes with respect to the antisymmetric modes of a suspended cable, the antisymmetric modes exhibit hardening behaviour only. Quadratic nonlinearities do however influence symmetric modes, where a softening-hardening behaviour results, as demonstrated by Luogno et al [1982], depending on the cable parameters. The nonlinear frequency amplitude relationship was developed and indicated that the point of modal cross-over where the first symmetric and antisymmetric modes coalesce became dependent on the amplitude of motion. Al-Noury and Ali[1985] presented a similar analysis, focussing on cables with small sag to span ratios. Their study included the out-of-plane co-ordinate in the equations of motion. This study concentrated on describing the resulting nonlinear behaviour due to excitation in the horizontal plane, excitation in the vertical plane, and excitation in the horizontal plane such that primary resonance occurred, when the transverse and vertical linear natural frequencies are closely spaced. Similar observations were made concerning the dependence of the softening, hardening behaviour on the cable parameters. The last case studied indicated the presence of strong coupling between the in-plane and out-of-plane modes, and the potential complexity of the ensuing response. Takahashi and Konishi[1987a] examined this problem further, and extended the analysis to include the three dimensional behaviour of arbitrarily inclined cables with arbitrary sag to span ratios. A Galerkin approach was adopted for the spatial domain, whilst the method of harmonic balance accounted for the temporal domain. The analysis investigated the free response of the cable, and hence defined the nonlinear frequency of vibration as a function of the amplitude of in-plane and out-of-plane initial deformations. The analysis confirmed that the in-plane behaviour exhibited a generally hardening response, although softening behaviour could be achieved depending on the system parameters. Due to the nonlinear coupling between the in-plane and out-of-plane equations of motion, where in-plane terms behave as coefficients in the out-of-plane equation of motion, out of plane response due to an in-plane excitation would result from bifurcation or parametric instability. Conversely, out-of-plane terms occur independently in the in-plane equation of motion, thus providing direct

excitation of the in-plane response due to out-of-plane excitation. This is confirmed by the analysis of Luogno et al [1982], where out-of-plane monofrequent oscillations were strongly coupled to in-plane motion. Consequently, out-of-plane excitation of a cable results in three dimensional motion, and thus the nonlinear out of plane behaviour is influenced by the in-plane response. In the second part of the study, Takahashi and Konishi[1987b], the stability of the out-of-plane response due to in-plane excitation was examined. It was demonstrated that the stability regions associated with the out-of-plane vibrations, occurred due to parametric excitation via the nonlinear coupling terms. Thus this analysis examined the parametric stability of the out-of-plane motion and concluded that in the general case both simple and sum type combination parametric resonances occurred⁶. The existence of the stability regions was shown to be dependent on the cable parameters, and on the symmetry of the excitation, which dictates the symmetry of the response and hence the importance of the cable curvature. In this regard, it was demonstrated that in the case of a horizontally supported sagged cable subjected to a symmetric excitation (quadratic nonlinearities included), as opposed to an antisymmetric excitation (quadratic nonlinearities excluded), the stability chart could be significantly different. In the latter, principal simple parametric resonances of symmetric modes do not arise. In the case of an inclined cable, the asymmetry of the profile resulted in the occurrence of all types of instability regions, irrespective of the forcing function. Benedettini and Rega[1987] presented a further study, employing a perturbation method, to investigate the planar behaviour of a horizontal cable with initial sag to in-plane primary resonance. It was concluded that the cable was most sensitive to cubic nonlinearities when its parameters conformed to those of a taut string, and thus hardening behaviour was observed, with one unstable and two stable periodic solutions. When a sagged configuration was analysed, it was evident that the quadratic nonlinearities lead to a softening-hardening behaviour, and consequently up to five periodic solutions may exist close to resonance. The sensitivity of the system to initial conditions was demonstrated by a numerical simulation of the equations of motion. Rega and Benedettini[1989a, 1989b], pursued their study further, by examining the superharmonic and subharmonic behaviour⁷ of a cable to in-plane excitation, for cables with various sag to span ratios. The studies demonstrated that the second order superharmonic produces notably stronger effects generally. This behaviour is accentuated by increased curvature or more

⁶Simple parametric resonances occur at intervals $2\omega_i/n$, where ω_i represents the linear natural frequency. A principal region is defined by $n = 1$, and secondary and tertiary regions follow $n = 2, 3$ respectively. A sum type combination resonance occurs in the intervals $(\omega_i + \omega_j)/n$, $n = 1, 2, 3, \dots$

⁷In this context, subharmonic refers to the situation where the response frequency is a subharmonic of the excitation frequency, the converse applying for the superharmonic case. A second order and third order subharmonic would arise when response occurs at $\Omega/2$ or $\Omega/3$ respectively, where Ω represents the excitation frequency.

dominant quadratic nonlinearity in the equations of motion.

Perkins[1992a] presents a study of the nonlinear modal interactions in a sagged cable when it is excited tangentially to the equilibrium profile, at one support. This study examines the condition whereby the first symmetric in-plane mode tunes to twice the first symmetric out of plane mode, and consequently an internal resonance exists. The longitudinal excitation was tuned to excite a principal parametric resonance of the out-of-plane mode, and due to the internal resonance, this excitation could simultaneously excite primary external resonance of the in-plane mode. Perkins[1992a] demonstrated that the cable response was either planar or highly coupled. A two degree of freedom model was applied to examine the stability of the planar and nonplanar motions⁸. The bifurcation condition governing planar stability indicated that the presence of the internal resonance greatly reduces the planar stability and enhances nonplanar response. It was also found that the principal parametric resonance disrupted the saturation phenomenon that would normally occur in the case of primary external resonance alone. The theoretical model provided a good qualitative description of the experimental behaviour observed in a laboratory exercise. It was demonstrated that a small support motion could induce substantial out-of-plane motion. Perhaps it is pertinent to note that the mine hoist system lends itself to combinations of tuning of a similar nature, with respect to the longitudinal and lateral modes, and the excitation. This aspect will be elaborated further in later chapters.

⁸Perkins notes that this condition of tuning coincides with the modal cross-over, and therefore the first in-plane symmetric and antisymmetric modes, and the second out-of-plane mode occur simultaneously. If the system was excited to induce principal parametric resonance of these modes, a truncated two degree of freedom model would not apply.

2.7 Conclusion

The purpose of this chapter was to establish an overall perspective of various aspects of the nonlinear dynamic nature of a suspended cable or taut string, and thereby reflect the depth and diversity of the subject. It is clear on reviewing the literature that a structural cable provides a remarkably good vehicle for the study of nonlinear dynamics. Recent research (Molteni [1990], O'Reilly and Holmes [1992]) confirms that chaotic motion has been observed in a taut stationary string, and this will no doubt stimulate further research. The particular studies reviewed were applied to a cable or string fixed at its extremities, and for this reason the results are not directly applicable to a mine hoist system. Many other studies exist concerning aspects of taut string and cable vibrations which are not considered pertinent to this thesis. For instance studies regarding the response of a taut string to travelling loads (Rodeman[1976], Sagartz[1975], Schultz[1968]), or where the string or cable supports a discrete mass (Rosenthal[1981], Smith[1964], Wickert[1988]). An interesting application regarding the effect of Coriolis coupling on a moving string resulted in a vibrating string being considered as a basis for the development of an angular motion sensor (Quick [1964]), and consequently the consideration of nonlinear effects and methods to quench these (Dimeff et al. [1966]).

Issues pertinent to the mine hoist system, namely the potential importance of cable curvature, transport velocity, nonlinear cable stretch and longitudinal inertia, require assessment in light of the literature reviewed.

Considering the Kloof Mine system, which is typical of many shafts in South Africa, the sag to span ratio⁹ varies between 1:100 and 1:500, whilst the non-dimensional cable stiffness parameter¹⁰ λ^2 varies between $\lambda^2 \approx 4$ to $\lambda^2 \approx 0.03$ for an empty skip at shaft head to a fully laden skip at shaft bottom respectively. The small sag to span ratios typically encountered on mine hoist systems justifies Mankowski's treatment of the catenary as a horizontally supported truncated catenary symmetrical about its mid point. This approximation will be applied in this thesis. In terms of the cable parameter, and with reference to Irvine's results [1981], the natural frequency of the first in-plane mode at shaft head, with an empty skip will be in error by approximately 15%, whilst the higher frequencies will be unaffected. On the ascending cycle, when the skip is at shaft head, this ratio is of the order of $\lambda^2 \approx 0.3$ and thus the in-plane natural frequencies of the cable will be well predicted by classical

⁹The sag to span ratio is given as $(d : l) = \frac{mg \cos(\theta)}{5H}$, where H is the horizontal component of tension, m the mass per unit length, l the span length, and θ the angle of inclination.

¹⁰Kloof Mine system parameters are $H = 80 - 340 \text{ kN}$, $m = 8.5 \text{ kg/m}$, $l = 75 \text{ m}$, $E = 1.1 \times 10^{11}$, $A = 1.02 \times 10^{-3}$, $\theta = 50^\circ$

tant string theory. Since the dominant lateral excitation is in the out-of-plane direction, avoidance of a directly excited mode could be assessed by considering the linear lateral natural frequencies of the catenary. However, since cable curvature provides coupling between the in-plane and out-of-plane motion, as demonstrated by Luogno et al[1982], Takahashi and Konishi [1987a],[1987b], Perkins [1992a], curvature is an important parameter to include in a numerical simulation.

With regard to the transport velocity of the cable, the effect on the linear natural frequencies is small, causing frequency changes of less than 2%. For this reason, it has been neglected in previous analyses (Dimitriou and Whillier [1973], Mankowski [1982]) of mine hoist systems. Although the lateral natural frequencies of the catenary are not strongly influenced by the Coriolis force developed, it is noted that if a real normal mode method is applied for the purpose of a numerical simulation, then a realistic simulation would dictate the inclusion of this effect. This occurs since the actual mode shapes associated with a travelling medium are complex, and consequently in the context of a real normal mode solution, implies that the Coriolis force couples and excites the higher modes resulting in a nonsynchronous behaviour.

A number of the studies presented regarding strings and cables with pinned end conditions neglected the longitudinal inertia, due to the large difference between the longitudinal and lateral wave speeds. In the context of the mine hoist system, the longitudinal wave speed is far greater than the lateral wave speed, however the longitudinal response is dictated by the modal response of the coupled system, and thus modal interaction between the transverse and longitudinal modes of the system must be accommodated.

Since the intention of this study is to examine the steady state stability of the stationary system as well as to develop a numerical simulation to account for the nonstationary nature of the system, the equations should be developed to account for transport velocity, catenary curvature and nonlinear stretch of the cable. These equations can then be simplified where appropriate as the thesis develops.

Chapter 3

Equations of Motion

3.1 Introduction

The purpose of this chapter is to develop the equations of motion of the coupled system. The coupled system refers to the catenary, headsheave, conveyance, and the coupling which exists between the catenary and the vertical rope. Mankowski[1982] attempted a lumped parameter numerical simulation of the mine hoist system by accounting for curvature and nonlinear rope stretch in the catenary, and coupling the catenary motion inertially through the headsheave to longitudinal motion in the vertical rope. It is preferred to achieve the description of the system in a more theoretical manner, by applying a continuum mechanics approach as developed by Luogno et al[1984], and later applied by Perkins and Mote[1987]. In this approach, the Lagrangian function of the system is formulated, and Hamilton's principle is applied to define the nonlinear equations of motion of the system. Since the definition of the Lagrangian function depends on the strain measure adopted, and the boundary conditions assumed, simplifications introduced are clearly evident in the theoretical development. This is considered to provide an advantage over a purely numerical approach as developed by Mankowski[1982], as it allows for an appreciation of the resulting equations of motion in terms of conventional techniques applied in nonlinear dynamics. To facilitate the development, the methodology applied by Perkins and Mote[1987] in deriving the equations of motion applicable to a sagged travelling cable, is presented. This approach is then extended to the mine hoist system, where the appropriate boundary conditions are accounted for. The full nonlinear equations of motion, consistent with the strain measure adopted are presented, where further truncation is applied as appropriate in later chapters.

3.2 The Sagged Travelling Catenary

3.2.1 Equations of Motion

A sagged, travelling elastic cable passing between two fixed eyelets is illustrated in figure (3.1). The cable is treated as a one dimensional continuum, located in the vertical $X_1 - X_2$ plane with gravity, g , aligned with the $-\underline{e}_2$ direction. The cable passes from the static equilibrium configuration χ^i to a final configuration χ^f during the motion. The unstretched or natural state is defined by χ^{o1} . The cable has a cross sectional area and transport velocity of A^o and c^o in the natural state χ^o , a modulus of elasticity E , and a mass density of ρ . The equilibrium configuration is defined by the position vector $\underline{R}^i(S^i, t)$ where S^i is the arc length co-ordinate referenced to the equilibrium configuration. Unit vectors in the equilibrium configuration are $\underline{t}^i, \underline{n}^i, \underline{b}^i$ in the tangential, normal and bi-normal directions respectively. The final configuration is defined by $\underline{R}^f(S^i, t) = \underline{R}^i(S^i, t) + \underline{U}(S^i, t)$ where $\underline{U}(S^i, t)$ represents the three dimensional motion of the final configuration, with respect to the equilibrium profile. The motion of a cable particle which includes the particle transport velocity $c^f \underline{t}^f$ is illustrated in figure 3.1. Thus:

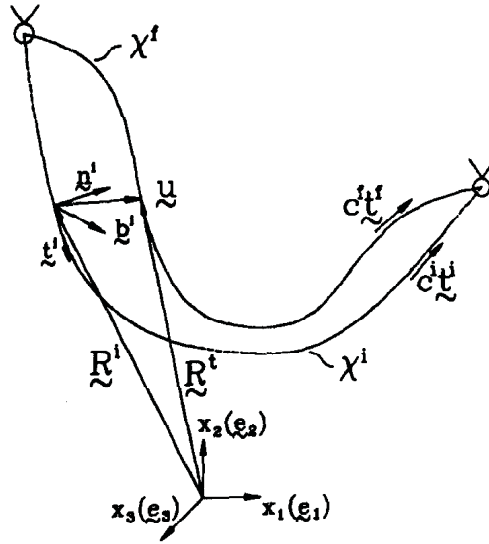


Figure 3.1: Catenary configuration

¹The purpose of introducing the natural or unstressed state, facilitates the extraction of the equations describing the equilibrium profile of the catenary from the equations of motion.

$$\underline{R}^f(S^i, t) = \underline{R}^i(S^i, t) + \underline{U}(S^i, t) \quad (3.1)$$

The motion $\underline{U}(S^i, t)$ is defined in the tangential, normal and bi-normal directions of the equilibrium configuration as:

$$\underline{U}(S^i, t) = u\mathbf{\underline{t}}^i + v\mathbf{\underline{n}}^i + w\mathbf{\underline{b}}^i$$

The cable is considered as a one dimensional continuum in the $\mathbf{\underline{t}}^i$ direction. Second order deformation effects are accounted for by utilising the $\mathbf{\underline{t}}^i$ component of the Green-Lagrange strain tensor. Luogno et al[1984], Perkins and Mote[1987] define the Lagrangian strain in the final configuration as:

$$e^f = \frac{1}{2} \left[\left\{ \frac{\partial}{\partial S^o} R^f(S^i, t) \right\}^T \cdot \left\{ \frac{\partial}{\partial S^o} R^f(S^i, t) \right\} - 1 \right]$$

where S^o denotes the arc length of the unstressed cable configuration. The Lagrangian strain in terms of the initial differential element dS^o and the final element dS^f is defined as $e^f = \frac{1}{2} \left[\frac{(dS^f)^2 - (dS^o)^2}{(dS^o)^2} \right]$. Introducing an intermediate equilibrium state, dS^i results in the strain measure e^f :

$$e^f = e^i + \left(\frac{dS^i}{dS^o} \right)^2 \epsilon$$

The Lagrangian strain resulting from a deformation from the equilibrium configuration χ^i to the final configuration χ^f is defined as ϵ :²

$$\epsilon = u_{,s} - \kappa v + \frac{1}{2} \{ u_{,s}^2 + v_{,s}^2 + w_{,s}^2 \} + \kappa \{ uv_{,s} - vu_{,s} + \frac{1}{2} \kappa (u^2 + v^2) \}$$

²The following manipulation is required:

$$e^f = e^i + \frac{1}{2} \left[\left\{ \frac{\partial}{\partial S^i} \underline{U}(S^i, t) \right\}^T \cdot \left\{ \frac{\partial}{\partial S^i} \underline{U}(S^i, t) \right\} + 2 \left\{ \frac{\partial}{\partial S^i} \underline{U}(S^i, t) \right\}^T \cdot \mathbf{\underline{t}}^i \right] \left(\frac{dS^i}{dS^o} \right)^2$$

where: $\underline{U}(S^i, t) = u\mathbf{\underline{t}}^i + v\mathbf{\underline{n}}^i + w\mathbf{\underline{b}}^i$
 and : $\frac{\partial \mathbf{\underline{t}}^i}{\partial S^i} = \kappa \mathbf{\underline{n}}^i$ $\frac{\partial \mathbf{\underline{n}}^i}{\partial S^i} = -\kappa \mathbf{\underline{t}}^i$ $\frac{\partial}{\partial S^i} R^i(S^i, t) = \mathbf{\underline{t}}^i$
 $\frac{\partial}{\partial S^i} \underline{U}(S^i, t) = (u_{,s} - \kappa v)\mathbf{\underline{t}}^i + (v_{,s} + \kappa u)\mathbf{\underline{n}}^i + w_{,s}\mathbf{\underline{b}}^i$

in which $(\mathfrak{B})_{,s}$ denotes partial differentiation with respect to S^i and κ refers to the curvature of the equilibrium configuration χ^i .

The Lagrangian strain may be formulated in a more direct manner by considering the deformation associated with a differential element in χ^f , referenced to a differential element in χ^i . Figure 3.2 presents a differential element of the cable in the $u-w$ and $u-v$ plane, with curvature κ , deformed from the equilibrium profile χ^i to the final profile χ^f . The differential length of the element in the final configuration can be calculated by considering the projection of the element onto the three orthogonal cartesian planes defined by X_1, X_2, X_3 :

$$(dS^f)^2 = [dS^i + u_{,s}dS^i - (v + v_{,s}dS^i)d\theta]^2 + [v_{,s}dS^i + (u + u_{,s}dS^i)d\theta]^2 + (w_{,s}dS^i)^2$$

Since $d\theta = \kappa dS^i$, and $\epsilon = \frac{1}{2} \frac{(dS^f)^2 - (dS^i)^2}{(dS^i)^2}$, and neglecting the differential products $v_{,s}dS^i d\theta, u_{,s}dS^i d\theta$ which vanish in the limit $dS^i \rightarrow 0$, the Green-Lagrange strain ϵ can be derived.

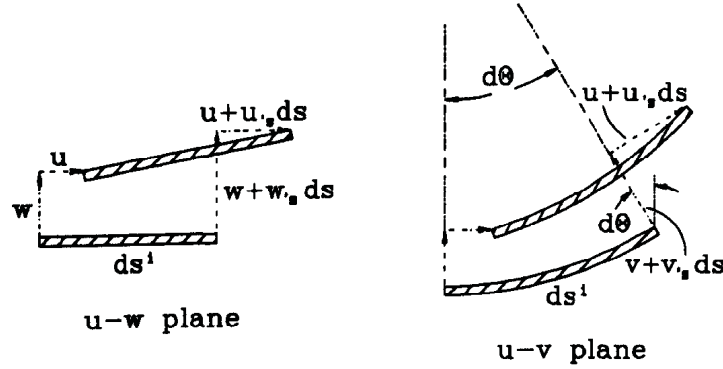


Figure 3.2: Displacement of a differential element of cable from χ^i to χ^f

3.2.2 Hamilton's Principle

In order to apply Hamilton's principle, the action integral is formulated as a combination of the kinetic energy π_V^f , the strain energy π_ϵ^f , and the gravitational potential energy π_g^f of the system. The action integral is stated as:

$$I = \int_{t_0}^{t_1} (\pi_V^f - \pi_\epsilon^f - \pi_g^f) dt$$

The strain energy of the cable π_ϵ^f in the final configuration χ^f formulated in terms of the equilibrium strain energy π_ϵ^i of the cable in the equilibrium configuration χ^i is:

$$\pi_\epsilon^f = \pi_\epsilon^i + \int_0^l (P^i + \frac{1}{2} A^i E \epsilon) \epsilon dS^i$$

where P^i represents the tension in the cable in the static equilibrium state χ^i . This represents a reduced form applied by Perkins and Mote[1987] to the more complete derivation provided by Luogno et al[1984]. It implies that $\frac{dS^i}{dS^o} \approx 1$, and thus the deformation of the cable from its unstretched length to the static equilibrium profile is in-elastic. This assumption is well justified for practical cables as can be ascertained by considering the constitutive law for a uniaxial cable: $P^i = EA^o \epsilon^i$, where $\epsilon^i = \frac{1}{2} [(\frac{dS^i}{dS^o})^2 - (\frac{dS^o}{dS^o})^2]$, $\frac{dS^i}{dS^o} = [1 + \frac{2P^i}{EA^o}]^{\frac{1}{2}}$. For practical cables $\frac{P^i}{EA^o} \ll 1$, and consequently the approximation $\frac{dS^i}{dS^o} \approx 1$ is justified. Since conservation of momentum and mass requires that $c^i A^i = c^o A^o$ and $A^i dS^i = A^o dS^o$, it follows that by the same argument A^i and c^i may be treated as constants.

The kinetic energy of the cable in the final configuration χ_V^f , referenced to the equilibrium configuration χ_V^i , is formulated as:

$$\pi_V^f = \int_0^l \frac{1}{2} \rho A^i \underline{V}^f \cdot \underline{V}^f dS^i$$

The velocity of the cable \underline{V}^f in the final configuration χ^f , may be obtained in terms of the equilibrium configuration χ^i , as follows:

$$\underline{V}^f(S^i, t) = \frac{d}{dt} [\underline{U}(S^i, t)] + c^i \underline{U}^f$$

$$\underline{t}^f = \frac{\partial}{\partial S^f} [R^f(S^i, t)] = \frac{\partial}{\partial S^i} [\underline{R}^i(S^i, t) + \underline{U}(S^i, t)] \frac{dS^i}{dS^f}$$

$$\underline{t}^f = [\underline{k}^i + \frac{\partial}{\partial S^i} \underline{U}(S^i, t)] \frac{dS^i}{dS^f}$$

The term $\frac{dS^i}{dS^f}$ is defined by considering the conservation of mass and momentum of a cable element:

$$A^i dS^i = A^f dS^f$$

$$A^i c^i = A^f c^f$$

$$\longrightarrow \frac{dS^i}{dS^f} = \frac{c^i}{c^f}$$

Thus the velocity of the cable, referenced to the equilibrium profile may be formulated as:

$$\longrightarrow \underline{V}^f(S^i, t) = c^i \underline{k}^i + c^i \frac{\partial}{\partial S^i} \underline{U}(S^i, t) + \frac{d}{dt} \underline{U}(S^i, t)$$

The gravitational potential energy π_g^f of the cable in its final configuration χ^f , written in terms of the gravitational potential energy π_g^i of the cable in the equilibrium configuration χ^i is:

$$\pi_g^f = \pi_g^i + \int_0^{l''} (u l_t + v l_n) \rho g A^i dS^i$$

where l_t, l_n are the components of the normal and tangential unit vectors projected on the vertical cartesian unit vector \underline{e}_2 , $\underline{e}_2 = l_t \underline{k}^i + l_n \underline{\Pi}^i$.

The equations of motion are determined by applying Hamilton's Principle, which requires stationarity of the action integral for arbitrary variations $\delta \underline{U}(S^i, t)$, vanishing at the limits t_0, t_1 .

$$\delta \left\{ \int_{t_0}^{t_1} (\pi_t^f - \pi_c^f - \pi_g^f) dt \right\} = 0 \quad (3.2)$$

On applying the condition of stationarity with respect to arbitrary variations $\delta \underline{U}(S^i, t)$, the above equation reduces to:

$$\delta I = \int_{t_0}^{t_1} \int_0^n \left[\frac{\partial \mathcal{L}}{\partial \underline{U}} \delta \underline{U} - \left(\frac{\partial \mathcal{L}}{\partial \underline{U}} \right) \frac{\partial}{\partial t} (\delta \underline{U}) - \frac{\partial \mathcal{L}}{\partial \underline{U}'} \frac{\partial}{\partial S^i} (\delta \underline{U}) \right] dS^i dt$$

where:

$$\mathcal{L}(\underline{U}, \underline{U}', \dot{\underline{U}}) = \frac{1}{2} \rho A^i \underline{V}^I \cdot \underline{V}^I - (P^i + \frac{1}{2} A^i E \epsilon) \epsilon - \rho g A^i (u l_t + v l_n)$$

Integration by parts with respect to t in the second term and S^i in the third, leads to:

$$\delta I = \int_{t_0}^{t_1} \left[\int_0^n \left[\frac{\partial \mathcal{L}}{\partial \underline{U}} - \frac{\partial}{\partial t} \left(\frac{\partial \mathcal{L}}{\partial \underline{U}} \right) - \frac{\partial}{\partial S^i} \left(\frac{\partial \mathcal{L}}{\partial \underline{U}'} \right) \right] \delta \underline{U} dS^i \right] + \left(\frac{\partial \mathcal{L}}{\partial \underline{U}'} \delta \underline{U} \right)_0^n dt$$

If the cable passes through fixed eyelets, as in the analysis of Perkins and Mote[1987], then $\delta \underline{U}|_0^n$ vanishes at the eyelets and consequently the last term in the above equation vanishes. Thus the equations of motion are obtained by satisfying Hamilton's principle by setting the integrand identically to zero. Perkins and Mote[1987] obtained the following equations of motion.

4 Component

$$\left[(P^i + A^i E \epsilon) a_1 \right]_{,s} - \left[(P^i + A^i E \epsilon) a_2 \right] - \rho H \epsilon = \left[\rho A^i (u_{,t} + c^i a_2) \right]_{,t} + \left[\rho A^i c^i (u_{,t} + c^i a_2) \right]_{,s} - \rho A^i c^i a_1 \left[v_{,t} + c^i a_2 \right]$$

3 Component

$$\left[(P^i + A^i E \epsilon) a_2 \right]_{,s} + \left[(P^i + A^i E \epsilon) a_3 \right] - \rho g \epsilon = \left[\rho A^i (u_{,t} + c^i a_2) \right]_{,t} + \left[\rho A^i c^i (u_{,t} + c^i a_2) \right]_{,s} - \rho A^i c^i a_1 \left[u_{,t} + c^i a_2 \right]$$

2 Component

$$\left[(P^i + A^i E \epsilon) a_3 \right]_{,s} = \left[\rho A^i (u_{,t} + c^i a_2) \right]_{,t} + \left[\rho A^i c^i (u_{,t} + c^i a_2) \right]_{,s}$$

where $a_1 = 1 + u_{,s} + w$, $a_2 = v_{,s} + w$ and $a_3 = w_{,s}$.

The equations of static equilibrium are extracted by setting the time derivatives and displacement components u, v, w to zero. Thus the equations governing the static equilibrium profile are:

$$-[(\rho A^i c^i) c^i]_{,s} + P^i_{,s} = \rho g A^i t_s$$

$$-\rho A^i \kappa (c^i)^2 + \kappa P^i = \rho g A^i t_n$$

Perkins and Mote[1987] show that by considering a momentum balance between the natural configuration χ^o and the equilibrium configuration χ^i , when the cable is stationary, a description of the equilibrium configuration results which is identical to that of the inelastic catenary solution in elementary statics. On linearising the equations of motion about the equilibrium profile, and retaining only first order terms in the displacements, Perkins and Mote[1987] determined the natural frequencies of a shallow sag, inclined travelling cable.

3.3 The Mine Hoist System

In the case of the mine hoist system, the boundary conditions differ from those applied to cables pinned at each end. Figure 3.3 represents the model of the mine hoist system analysed. In this figure, the catenary refers to the section of rope between the winder drum and sheave wheel. In practice, the static tension in the catenary is high, and consequently the asymmetry due to the cable inclination is small. The catenary profile is flat and lies close to the chord between the drum and sheave. The sag to span ratio at the mid point of the chord, where the sag is measured perpendicular to the chord, is of the order of 1:100 or less. In this regard it is acceptable to treat the cable as a flat sag cable, by neglecting variations in the tension and treating the curvature as constant. This results in a symmetric parabolic cable equilibrium profile, where the inclination of the cable is accounted for by modifying the gravitational constant to $g\cos(\theta)$, where θ represents the angle of inclination of the chord from the horizontal axis³. Initially the equations of motion are developed to account for the general case of an inclined sagged catenary as illustrated in figure 3.3. Subsequent simplification of the equations of motion is introduced, on the basis of assuming constant tension and curvature, leading to the equilibrium profile of a flat sag parabolic cable.

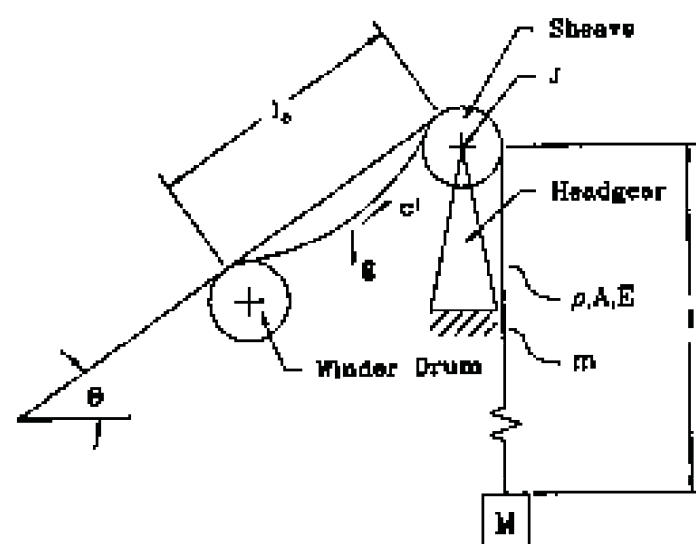


Figure 3.3: Mine hoist configuration

³Mankowski[1982] made a similar simplification, justified on the basis that the variation in axial tension due to the inclination of the cable is small in comparison to the static tension, hence a symmetric parabolic catenary was employed in his analysis.

The system parameters are the catenary length l_c , the total rope length l_v , the material density of the cable ρ , the linear mass density of the cable m , the cross-sectional area of the cable A , the elastic modulus of the cable E , the sheave wheel mass moment of inertia J , the mass of the skip and pay load M , and the transport velocity c^1 .

The boundary condition at the drum end is treated as pinned. Thus the winder is considered as a perfect power source, and dynamic interaction between the winder and hoist system is neglected⁴. The sheave end boundary condition represents the fundamental difference between studies regarding strings and cables and the mine hoist system. In this study the coupling between the catenary motion and the vertical rope is accommodated. To simplify the analysis, it is assumed that the catenary-sheave-vertical rope interface is accounted for by a rigid band passing over the sheave. The catenary is attached to this band, which admits motion tangential to the equilibrium profile. Thus the catenary is effectively supported by frictionless rollers at the sheave, such that lateral motion at the point of attachment to the band is eliminated, as illustrated in figure 3.4. This effectively couples the sheave inertially to the longitudinal system response⁵. Although lateral movement of the vertical rope occurs in practice through autoparametric excitation due to the catenary motion, only longitudinal motion of the vertical rope is admitted. Thus the model proposed is ultimately identical to that implemented numerically by Mankowski[1982]. The aspect of including lateral motion of the vertical rope is viewed as a future research incentive.

The definition of the dynamic response of this model requires equations of motion describing the three dimensional motion of the catenary, the motion of the sheave wheel, and the longitudinal motion of the vertical rope and skip. Figure 3.4 illustrates the variables $u(s,t)$, $v(s,t)$, $w(s,t)$ which represent the motion at a station along the catenary in the tangential, normal and bi-normal direction of the equilibrium profile respectively, where s refers to the arc length co-ordinate measured along the equilibrium configuration. The co-ordinates u_1 , $\bar{u}(s,t)$, u_2 represent the tangential motion at the sheave, the longitudinal motion of the vertical rope, and the motion at the skip respectively. Continuity of motion across the sheave requires $u(l_c,t) = u_1 = \bar{u}(l_c,t)$.

⁴This is a significant assumption which was introduced to simplify the analysis at this stage of the research. Kaczmarczyk[1993] is considering the effect of including the electrical characteristics of the winder motor.

⁵Appendix M presents an alternative formulation, where the kinematics of the cable sheave contact are defined through geometric considerations, resulting in constraint relationships governing the motion of the cable at the sheave end.

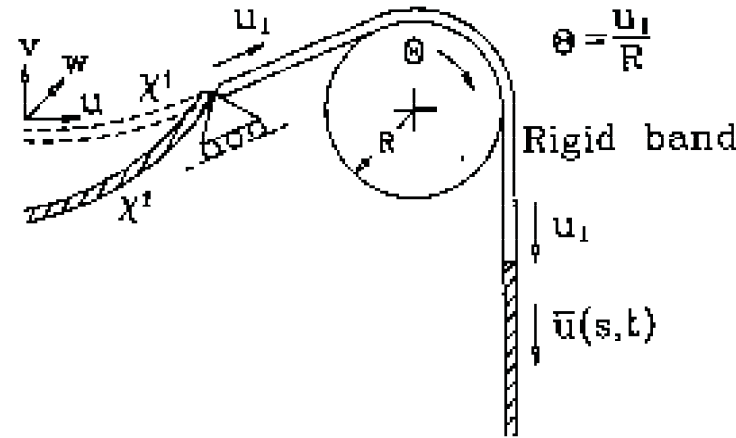


Figure 3.4: Catenary - sheave interface

3.3.1 Equations of Motion and Equilibrium

The equations of motion are developed for the system described, by following a similar development to that of Perkins and Mote[1987]. The kinetic, elastic and gravitational potential energy of the system is defined in terms of the equilibrium state of the system. The equations of motion are extracted via Hamilton's principle. By setting displacements and time derivatives to zero the equations defining the equilibrium state of the system result.

In this analysis the Lagrangian strain ϵ defines the strain measure in the catenary:

$$\epsilon = u_{,s} - \kappa v + \frac{1}{2} \{u_{,s}^2 + v_{,s}^2 + w_{,s}^2\} + \kappa \{uv_{,s} - vu_{,s} + \frac{1}{2} \kappa (u^2 + v^2)\}$$

Since lateral motion is not permitted in the vertical rope, the strain measure applied in the vertical rope $\bar{\epsilon}$ is defined as:

$$\bar{\epsilon} = \bar{u}_{,s}$$

The strain energy of the cable π_c' in the final configuration, formulated in terms

of the equilibrium strain energy π_e^i of the cable in the equilibrium configuration is:

$$\pi_e^f = \pi_e^i + \int_0^{l_c} (P^i + \frac{1}{2}AE\epsilon)\epsilon ds + \int_{l_c}^{l''} (\bar{P} + \frac{1}{2}AE\bar{\epsilon})\bar{\epsilon} d\bar{s}$$

where P^i, \bar{P} represent the tension in the catenary and vertical rope in the static equilibrium state respectively.

The kinetic energy of the cable in the final configuration, referenced to the equilibrium configuration is formulated as:

$$\pi_v^f = \int_0^{l_c} \frac{1}{2}\rho A^i \underline{V}^f \cdot \underline{V}^f ds + \int_{l_c}^{l''} \frac{1}{2}\rho A^i \bar{\underline{V}}^f \cdot \bar{\underline{V}}^f d\bar{s} + \frac{1}{2} \frac{I}{R^2} (\dot{u}_2 + c^i)^2 + \frac{1}{2} M (\dot{u}_2 + c^i)^2$$

where $\underline{V}^f, \bar{\underline{V}}^f$ represents the particle velocity of the rope in the catenary and vertical section respectively; $(\dot{u}_2 + c^i), (\dot{u}_2 + c^i)$ represent the tangential velocity at the sheave and skip respectively.

The velocity of the catenary \underline{V}^f in the final configuration is obtained as:

$$\underline{V}^f = \{c^i a_1 + u_{,t}\} \underline{t}^i + \{c^i a_2 + v_{,t}\} \underline{n}^i + \{c^i a_3 + w_{,t}\} \underline{b}^i$$

where: $a_1 \approx 1 + u_{,s} - \kappa v$, $a_2 \approx v_{,s} + \kappa u$, $a_3 \approx w_{,s}$.

The velocity of the vertical rope $\bar{\underline{V}}^f$ in the final configuration is obtained as:

$$\bar{\underline{V}}^f = \{c^i(1 + \bar{u}_{,s}) + \bar{u}_{,t}\} \bar{\underline{t}}^i$$

The gravitational potential energy π_g^f of the cable in the final configuration, written in terms of the gravitational potential energy π_g^i of the cable in the equilibrium configuration is:

$$\pi_g^f = \pi_g^i + \int_0^{l_c} (u_{,t} + v_{,t}) \rho g A^i ds - \int_{l_c}^{l''} \rho g A^i \bar{u} d\bar{s} - M g u_2$$

where l_i, l_n are the components of the normal and tangential unit vectors projected on the vertical cartesian unit vector \underline{e}_2 , $\underline{e}_2 = l_t \underline{t}^i + l_n \underline{n}^i$.

The Lagrangian of the system is thus:

$$\mathcal{L}(s, t, u, v, w, u_1, u_2, u_{,s}, v_{,s}, w_{,s}, \bar{u}_{,s}, u_{,t}, \dot{v}_{,t}, w_{,t}, \dot{u}_1, \dot{u}_2, \bar{u}_{,t}) = \pi_k^f - \pi_e^f - \pi_g^f$$

The Lagrangian is split into discrete and continuous components for convenience:

$$\begin{aligned} \mathcal{L}(s, t, u, v, w, u_{,s}, v_{,s}, w_{,s}, u_{,t}, v_{,t}, w_{,t}, \bar{u}, \bar{u}_{,s}, \bar{u}_{,t}, u_1, \dot{u}_1, u_2, \dot{u}_2) = \\ \mathcal{L}_1(s, t, u, v, w, u_{,s}, v_{,s}, w_{,s}, u_{,t}, v_{,t}, w_{,t}) \\ + \mathcal{L}_2(s, t, \bar{u}, \bar{u}_{,s}, \bar{u}_{,t}) + \mathcal{L}_3(t, u_1, \dot{u}_1) + \mathcal{L}_4(t, u_2, \dot{u}_2) \end{aligned}$$

where:

$$\begin{aligned} \mathcal{L}_1 &= \int_0^{l_c} [\\ &\int_{l_c}^{l_v} [\frac{1}{2} \rho A^i \underline{V}^f \cdot \underline{V}^f - (\bar{P}^i + \frac{1}{2} A^i E \bar{\epsilon}) \bar{\epsilon} + mg \bar{u}] ds \\ \mathcal{L}_3 &= \frac{1}{2} \frac{I}{R^2} (\dot{u}_1 + c^i)^2 \\ \mathcal{L}_4 &= \frac{1}{2} M (\dot{u}_2 + c^i)^2 + M g u_2 \end{aligned}$$

The equations of motion are determined by applying Hamilton's principle, which requires stationarity of the action integral for arbitrary variations in the dependent co-ordinates, compatible with the boundary conditions, which vanish at t_0, t_1 .

$$\delta \left\{ \int_{t_0}^{t_1} (\pi_V^f - \pi_e^f - \pi_g^f) dt \right\} = 0 \quad (3.3)$$

Applying the condition of stationarity with respect to arbitrary variations in the co-ordinates $\delta \underline{U}(s, t), \delta \bar{u}(s, t), \delta u_1, \delta u_2$, leads to the requirement that:

$$\begin{aligned} & \int_{t_0}^{t_1} \left[\int_0^{l_c} \left\{ \frac{\partial \mathcal{L}_1}{\partial \underline{U}} - \frac{\partial}{\partial t} \left(\frac{\partial \mathcal{L}_1}{\partial \dot{\underline{U}}} \right) - \frac{\partial}{\partial s} \left(\frac{\partial \mathcal{L}_1}{\partial \underline{U}'} \right) \right\} \delta \underline{U} ds + \frac{\partial \mathcal{L}_1}{\partial \underline{U}'} \delta \underline{U} \Big|_0^{l_c} \right. \\ & \quad + \int_{l_c}^{l_v} \left\{ \frac{\partial \mathcal{L}_2}{\partial \bar{u}} - \frac{\partial}{\partial t} \left(\frac{\partial \mathcal{L}_2}{\partial \dot{\bar{u}}} \right) - \frac{\partial}{\partial s} \left(\frac{\partial \mathcal{L}_2}{\partial \bar{u}'} \right) \right\} \delta \bar{u} ds + \frac{\partial \mathcal{L}_2}{\partial \bar{u}'} \delta \bar{u} \Big|_{l_c}^{l_v} \\ & \quad \left. + \left\{ \frac{\partial \mathcal{L}_3}{\partial u_1} - \frac{\partial}{\partial t} \left(\frac{\partial \mathcal{L}_3}{\partial \dot{u}_1} \right) \right\} \delta u_1 + \left\{ \frac{\partial \mathcal{L}_4}{\partial u_2} - \frac{\partial}{\partial t} \left(\frac{\partial \mathcal{L}_4}{\partial \dot{u}_2} \right) \right\} \delta u_2 \right] dt = 0 \end{aligned}$$

where:

$$\underline{U}^T(s, t) = \{u(s, t), v(s, t), w(s, t)\}$$

$$\delta \underline{U}^T(0, t) = \{0, 0, 0\}$$

$$\delta \underline{U}^T(l_c, t) = \{\delta u_1, 0, 0\}$$

$$\delta \bar{u}(l_c, t) = \delta u_1$$

$$\delta \bar{u}(l_v, t) = \delta u_2$$

Applying these conditions, the equations of motion result as:

$$\begin{aligned} \frac{\partial \mathcal{L}_1}{\partial \underline{U}} - \frac{\partial}{\partial t} \left(\frac{\partial \mathcal{L}_1}{\partial \dot{\underline{U}}} \right) - \frac{\partial}{\partial s} \left(\frac{\partial \mathcal{L}_1}{\partial \underline{U}'} \right) &= 0 \\ \frac{\partial \mathcal{L}_2}{\partial \bar{u}} - \frac{\partial}{\partial t} \left(\frac{\partial \mathcal{L}_2}{\partial \dot{\bar{u}}} \right) - \frac{\partial}{\partial s} \left(\frac{\partial \mathcal{L}_2}{\partial \bar{u}'} \right) &= 0 \\ \frac{\partial \mathcal{L}_3}{\partial u_1} - \frac{\partial}{\partial t} \left(\frac{\partial \mathcal{L}_3}{\partial \dot{u}_1} \right) + \frac{\partial \mathcal{L}_1}{\partial \underline{U}'} \Big|_{l_c} - \frac{\partial \mathcal{L}_2}{\partial \bar{u}'} \Big|_{l_c} &= 0 \\ \frac{\partial \mathcal{L}_4}{\partial u_2} - \frac{\partial}{\partial t} \left(\frac{\partial \mathcal{L}_4}{\partial \dot{u}_2} \right) + \frac{\partial \mathcal{L}_2}{\partial \bar{u}'} \Big|_{l_v} &= 0 \end{aligned}$$

Performing the necessary manipulations results in a set of six nonlinear differential equations defining the motion of the mine hoist system.

$$\left[(\dot{P}^i + A^i \kappa c^i) a_1 \right]_{,s} - \left[(\dot{P}^i + A^i \kappa c^i) a_2 \right] - \rho g l_1 = \left[\rho A^i (u_{,t} + c^i a_1) \right]_{,t} + \left[\rho A^i c^i (u_{,t} + c^i a_1) \right]_{,s} - \rho A^i c^i \kappa [u_{,t} + c^i a_2]$$

$$\left[(\dot{P}^i + A^i E c^i) a_2 \right]_{,s} + \left[(\dot{P}^i + A^i E c^i) a_3 \right] - \rho g l_2 = \left[\rho A^i (v_{,t} + c^i a_2) \right]_{,t} + \left[\rho A^i c^i (v_{,t} + c^i a_2) \right]_{,s} - \rho A^i c^i \kappa [u_{,t} + c^i a_1]$$

$$\left[(\dot{P}^i + A^i E c^i) a_3 \right]_{,s} = \left[\rho A^i (w_{,t} + c^i a_3) \right]_{,t} + \left[\rho A^i c^i (w_{,t} + c^i a_3) \right]_{,s}$$

$$[(\dot{P}^i + A^i E c^i)]_{,s} + m g = [\rho A^i (c^i a_3 + \bar{w}_{,t})]_{,t} + [\rho A^i c^i (c^i a_3 + \bar{w}_{,t})]_{,s}$$

$$\left[(\dot{P}^i + A^i E c^i) - (\dot{P}^i + A^i E c^i) a_1 \right]_{,t} = \rho A^i (c^i)^2 (\bar{w}_{,s} - w_{,s}) v_{,t} = \left[\frac{1}{R^2} (\dot{u}_1 + c^i) \right]_{,t}$$

$$M g + \rho A^i (c^i)^2 = \bar{P}^i(l_2) - [A^i E c^i]_{,t} = [M (\dot{u}_2 + c^i)]_{,t} = \rho A^i c^i a_2$$

$$\text{where } a_1 = 1 + u_{,s} + w_{,s}, \quad a_2 = v_{,s} + w_{,s}, \quad a_3 = w_{,s}, \quad a_4 = 1 + \bar{w}_{,s}.$$

The first three equations are identical to those derived by Perkins and Mote(1987). The fourth equation describes the longitudinal motion of the vertical rope. The fifth and sixth equations describe the inertial balance across the shrave, coupling the catenary to the vertical rope, and the boundary condition required to achieve dynamic equilibrium between the skip and the tail of the vertical rope, respectively.

The equations of static equilibrium, for a constant velocity state $\dot{c}_i^i = 0$, are extracted by setting the time derivatives and displacement components to zero. Thus the equations governing the static equilibrium profile are:

$$-[(\rho A^i c^i) c^i]_{,s} + P_{,s}^i = \rho g A^i l_i \quad (3.4)$$

$$-\rho A^i \kappa (c^i)^2 + \kappa P^i = \rho g A^i l_n \quad (3.5)$$

$$\bar{P}_{,s}^i + m g = 0 \quad (3.6)$$

$$P^i(l_a) - \bar{P}^i(l_c) = 0 \quad (3.7)$$

$$Mg + \rho A^i (c^i)^2 - \overline{P}^i(l_0) = 0 \quad (3.8)$$

Perkins and Mote[1987] solved the equilibrium equations governing the profile of a cable with arbitrary inclination and sag. This was accomplished by introducing a momentum balance across a segment of arc length S^i , extending from the the lowest point on the profile where the tension is P_0 , to any other station along the arc length where the tension is P^i ⁴. Referring to figure 3.5, the momentum balance yields:

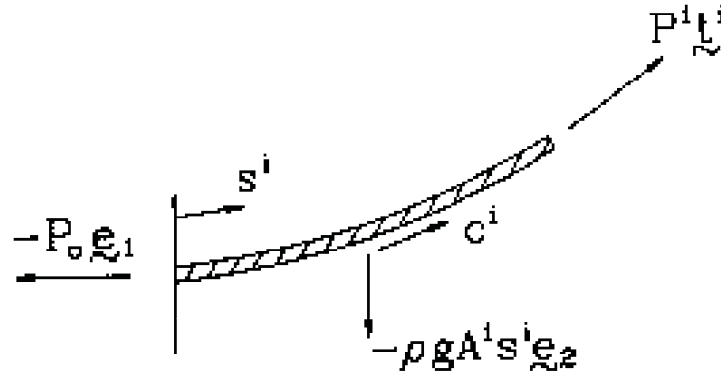


Figure 3.5: Control volume of segment of cable.

$$[P^i - \rho A^i c^{i2}] \underline{l}^i = [P_0 - \rho A^i c^2] \underline{e}_1 + \rho A^i g S^i \underline{e}_2$$

Since $\underline{l}^i = l_1 \underline{e}_1 + l_2 \underline{e}_2$, l_1, l_2 can be defined. Together with the first two equilibrium equations, the tension distribution and curvature can be defined as:

$$P^i(S^i) = [(P_0 - \rho A^i c^2)^2 + (\rho g A^i S^i)^2]^{\frac{1}{2}} + \rho A^i c^2$$

$$\kappa^i(S^i) = \rho g A^i (P_0 - \rho A^i c^2) / [(P_0 - \rho A^i c^2)^2 + (\rho A^i S^i)^2]$$

Integration of the cable curvature leads to:

$$X_2^i(X_1^i) = M^2 \cosh(X_1^i / M^2)$$

⁴The approximation $A^0 \approx A^i$ and $c^0 \approx c^i$ is introduced on the basis that $P^i / EA^0 \ll 1$.

and the arc length co-ordinate:

$$S^i = \int_0^{X_1^i} (1 + (\frac{dX_2^i}{dX_1^i})^2)^{\frac{1}{2}} dX_1 = M^2 \sinh(X_1^i/M^2)$$

where $M^2 = (P_o - \rho A^i c^i)/\rho g A^i$. The equation for the catenary profile $X_2^i(X_1^i)$ and the arc length S^i are used to define the tension P_o and the position of the catenary in the X_1, X_2 plane, given c^i , and the initial cable length L^i . Although this approach accurately accounts for the tension and curvature distribution in the equilibrium configuration, as noted previously, substantial simplification can be made in the context of the mine hoist system by treating the catenary as a flat sag cable.

3.3.2 Flat Sag Cable Approximation

In the mine hoist system, the catenary is inclined. However, due to the high tension in the catenary as a result of the payload and mass of the vertical rope, the cable profile lies close to the chord between the drum and sheave. Irvine[1981] derived the profile of a static inclined cable, under sufficient tension such that the profile lies close to the chord, as illustrated in figure 3.6. The approximate profile with respect to the chord is defined as:

$$z = \frac{1}{2}x(1-x)[1 - \frac{\epsilon}{3}(1-2x)]$$

where $z = z/(mgl^2 \cos(\theta)/H)$, $x = x/l$, $\epsilon = mgl \sin(\theta)/H$; z represents the perpendicular distance between the profile and the chord, x represents the distance from the upper support along the chord length, and H represents the component of the cable tension projected onto the chord at the upper support. This profile is asymmetric with respect to the mid span, where the asymmetry is dictated by the magnitude of ϵ . If $\epsilon \ll 1$, the variation of the tension is considered to be negligible with respect to the static tension, and the profile may be approximated by a symmetric parabola with respect to its mid span⁷. By assuming such a profile, Irvine[1981] suggests that the natural frequencies of an inclined cable can be determined from the frequency equation of a flat sag horizontal cable, where the cable parameter is corrected

⁷The same solution is obtained by considering the cable to be supported at equal elevation, and correcting the gravitational constant to $g \cos(\theta)$.